

(1,1) ALMOST L-SPACE KNOTS

FRASER BINNS AND HUGO ZHOU

ABSTRACT. We give a diagrammatic characterization of the $(1,1)$ knots in the three-sphere and lens spaces which admit large Dehn surgeries to manifolds with Heegaard Floer homology of next-to-minimal rank. This is inspired by a corresponding result for $(1,1)$ knots which admit large Dehn surgeries to manifolds with Heegaard Floer homology of minimal rank due to Greene-Lewallen-Vafaee.

1. INTRODUCTION

Heegaard Floer homology is a powerful package of invariants due originally to Ozsváth-Szabó [OS04b]. A central question in the study of Heegaard Floer homology is whether or not any objects defined in terms of Heegaard Floer homology can be given Floer-free interpretations. We seek to address a special case of this question in this paper.

The simplest version of Heegaard Floer homology is a three manifold invariant, denoted $\widehat{\text{HF}}(-)$. If Y be a rational homology sphere then $\widehat{\text{HF}}(-)$ satisfies the following inequality:

$$(1) \quad \text{rank}(\widehat{\text{HF}}(Y)) \geq |H_1(Y; \mathbb{Z})|.$$

For example see [OS06, Lemma 1.6]. Here $|H_1(Y; \mathbb{Z})|$ is the cardinality of $H_1(Y; \mathbb{Z})$. An *L-space* is a rational homology sphere for which inequality (1) is tight. Examples include lens spaces. Conjecturally, L-spaces can be characterized as rational homology spheres either which do not admit taut foliations, or whose fundamental groups are not left orderable [Juh15, Conjecture 5]. *L-space knots* are the knots that admit large Dehn surgeries to L-spaces. L-space knots have played a key roll in work on the Berge conjecture [OS05] but are also of wider interest. An *almost L-space* is a rational homology sphere Y for which inequality (1) is “almost tight” – that is $\text{rank}(\widehat{\text{HF}}(Y)) = |H_1(Y; \mathbb{Z})| + 2$. Examples include the Brieskorn sphere $\Sigma(2, 3, 11)$. The term “almost L-space” was coined by Baldwin-Sivek in their work on the characterizing slopes of the knot 5_2 [BS22]. Almost L-spaces have also been studied in other contexts; for example Lin gives results concerning the Stein fillings of a subclass of almost L-spaces [Lin20].

Almost L-space knots are to almost L-spaces as L-space knots are to L-spaces:

Definition 1.1. An *almost L-space knot* is a knot K such that $S_n^3(K)$ is an almost L-space for an integer $|n| \geq 2g(K) - 1$ and K is not an L-space knot.

Here $S_n^3(K)$ indicates n -surgery on K . Examples of almost L-space knots include the mirror of 5_2 , $T(2, 3) \# T(2, 3)$, and $(2, 4g(K) - 3)$ -cables of L-space knots. Note that the only L-space knots such that $S_n^3(K)$ is an almost L-space for an integer $|n| \geq 2g(K) - 1$ are the trefoils. The first author proved that the CFK^∞ type of an almost L-space knot is either a staircase with a length one box or a so called “almost staircase” (See the discussion below Definition 2.2) [Bin23]. The $(2, 4g(K) - 3)$ cables of L-space knots are the only infinite family of almost L-space knots that have appeared in the literature, to the best knowledge of the authors. We give an infinite family of almost L-space knots in Corollary 1.6.

In this paper, we study rational homology spheres admitting genus one Heegaard splittings, namely S^3 and lens spaces. We consider L-space and almost L-space knots in these manifolds. Note that this definition is broader than the usual definition of (almost) L-space knots, which are required to be knots in S^3 . See the discussion below Definition 2.1.

A knot $K \subset Y$ is called a *(1,1) knot* if there is a genus one Heegaard splitting of Y such that K intersect each handlebody in a trivial arc. In other words, $(1,1)$ knots are precisely those that admit

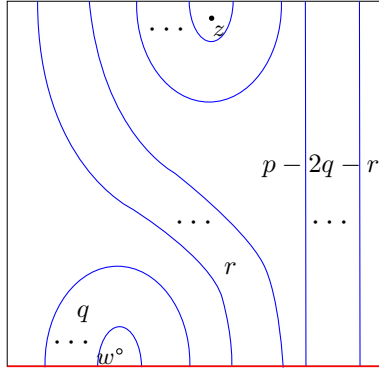


FIGURE 1. The standard $(1, 1)$ diagram for the four-tuple (p, q, r, s) by [Ras05], where $q, r \geq 0$, $2q + r \leq p$ and $0 \leq s < p$. There are q strands of “rainbow arcs” on both sides. If we label the intersection points on the top and bottom sides from left to right, then the i -th point on the top is identified with the $(i + s)$ -th point on the bottom.

a doubly-pointed genus one Heegaard diagram. Such a diagram is called a $(1, 1)$ *diagram*. The fact that $(1, 1)$ knots admit simple Heegaard diagrams makes their knot Floer homology comparatively easy to compute and as a result there are a number of results concerning the knot Floer homology of $(1, 1)$ knots in the literature [Ras05, GMM05, Rac15]. In particular, the knot Floer homology of $(1, 1)$ knots is computable [Doy05]. Despite this, there is no general formula for the knot Floer homology of $(1, 1)$ knots.

Figure 1 shows a *standard $(1, 1)$ diagram* by [Ras05], which can be encoded by a 4-tuple of integers (p, q, s, r) . See the beginning of Section 2.2 for details. Every $(1, 1)$ diagram can be uniquely isotoped to a standard diagram, so we will generally make statements regarding the associated standard diagram. We will be particularly interested in the orientations of the “rainbow arcs” which are those that bound bigons in Figure 1. If the rainbow arcs around a fixed basepoint are not oriented in the same direction, call the orientation in the minority the *inconsistent direction* and these rainbow arcs *inconsistent arcs*. (If there are the same number of arcs in each direction, choose either direction as the inconsistent direction.) Having no inconsistent arc means that all the rainbow arcs around a fixed basepoint are in the same direction.

Definition 1.2. ([GLV18, Definition 1.1].) A standard diagram is *coherent* if there are no inconsistent arcs.

This diagrammatic condition characterizes L-space knots amongst $(1, 1)$ knots:

Theorem 1.3. ([GLV18, Theorem 1.2].) *A standard diagram represents an L-space knot if and only if it is coherent.*

We seek to extend this result, via an extension of the techniques Greene-Vafaee-Lewallen use to obtain it, to the case of almost L-space $(1, 1)$ knots. It would have been natural to conjecture that the new diagrammatic condition required for this would be that there are exactly two inconsistent arcs in the associated standard diagram (one around each basepoint). However, this statement fails even for relatively simple $(1, 1)$ diagrams, see Figure 5. It turns out the appropriate definition is the following.

Definition 1.4. A standard diagram is *strongly almost coherent* if there are exactly two inconsistent arcs and one of the following is true: ¹

¹We call a standard diagram with the same number of arcs in each direction (so that there is a choice of inconsistent direction) strongly almost coherent if for a choice of inconsistent direction one of the conditions is satisfied.

Four-tuple (p, q, s, r)	Knot name
$(5, 2, 0, 1), (5, 2, 0, 4)$	4_1
$(7, 2, 0, 3), (7, 2, 0, 4), (7, 3, 0, 1)$ $(7, 3, 0, 2), (7, 3, 0, 5), (7, 3, 0, 6)$	5_2
$(11, 3, 1, 4)$	10_{139}
$(13, 4, 1, 7)$	$12n_{725}$
$(15, 3, 1, 4), (15, 4, 2, 5)$	$16n_{792631}$

TABLE 1. All the $(1, 1)$ almost L-space knots in S^3 with $\text{rank}(\widehat{\text{HFK}}(K)) \leq 15$, up to mirroring.



FIGURE 2. Two possible cases in Definition 1.4. The inconsistent arcs are the outermost arcs in the diagram on the right.

- the inconsistent arcs share a common end point;
- the inconsistent arcs are connected by two other rainbow arcs.

This condition turns out to be equivalent to having exactly two inconsistent arcs in the universal cover (a condition we call *virtually almost coherent*, see Definition 3.1.) We show that this characterizes almost L-space knots amongst $(1, 1)$ knots:

Theorem 1.5. *A standard diagram represents an almost L-space knot if and only if it is strongly almost coherent.*

In fact we prove a stronger statement; that the almost L-space knots that arise as $(1, 1)$ knots have the CFK^∞ -type of box plus staircase complexes, see Theorem 3.4. This implies that not every bigraded vector space that arises as $\widehat{\text{HFK}}(K)$ for some K arises as $\widehat{\text{HFK}}(K')$ for some $(1, 1)$ knot K' . This contrasts with the case of the decategorification of knot Floer homology – the Alexander polynomial, $\Delta_K(t)$. The Alexander polynomial has the property that any polynomial which arises as $\Delta_K(t)$ for some knot K arises as $\Delta_{K'}(t)$ for some $(1, 1)$ knot K' [Fuj96].

One can readily check by computer algorithm whether or not a given $(1, 1)$ diagram is strongly almost coherent; see Section 4 for the pseudo code. In Table 1, we have recorded all the four-tuples with $p \leq 15$ in S^3 that satisfies the strongly almost coherent condition. For each pair of the mirror four-tuples (p, q, r, s) and $(p, q, p - 2q - r, 2q - s)$ exactly one is recorded.

We also give a new infinite family of almost L-space knots. Let K_j be the $(1, 1)$ knot in S^3 given by the four-tuple $(7 + 4j, 3, 4j, 2)$ with $j \in \mathbb{Z}_{\geq 0}$.

Corollary 1.6. *Knot K_j is an almost L-space knot for $j \in \mathbb{Z}_{\geq 0}$.*

Proof. The diagram given by the four-tuple $(7 + 4j, 3, 4j, 2)$ (See Figure 12 (a)) is strongly almost coherent according to Definition 1.4. Therefore by Theorem 1.5 K_j is an almost L-space knot. \square

Let $\widehat{\mathcal{C}}_{\mathbb{Z}}$ denote the group of pairs (Y, K) , such that K is a knot in an integer homology sphere Y which bounds integer homology ball. The group action is given by connected sum. Let $\mathcal{C}_{\mathbb{Z}}$ denote the subgroup of $\widehat{\mathcal{C}}_{\mathbb{Z}}$ consisting of pairs (S^3, K) .

Proposition 1.7. *The family $\{K_j\}_{j \geq 0}$ satisfies the following properties.*

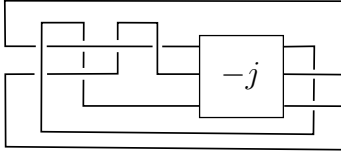


FIGURE 3. The knot diagram of K_j for $j \geq 0$. Here $-j$ indicates j left-handed full twists.

- (1) The family $\{(S_{+1}^3(K_j) \# -S_{+1}^3(K_j), \mu \# U)\}_{j>0}$ generates a \mathbb{Z}^∞ summand in $\widehat{\mathcal{C}}_{\mathbb{Z}}/\mathcal{C}_{\mathbb{Z}}$, where μ is the image of a meridian of K_j and U is the unknot;
- (2) K_j is not homology concordant to any L-space knot.

Previous examples of families of knots that generate \mathbb{Z}^∞ summands of the quotient group $\widehat{\mathcal{C}}_{\mathbb{Z}}/\mathcal{C}_{\mathbb{Z}}$ use L-space knots in the place of K_j , see [DHST21, Corollary 1.2, Lemma 11.3].

This paper is organised as follows; in Section 2 we review relevant aspects of Heegaard Floer homology and $(1, 1)$ knots while in Section 3 we prove Theorem 1.5 and Proposition 1.7. In Section 4 we give an algorithm for checking if a $(1, 1)$ diagram is strongly almost coherent.

Acknowledgments. The first author would like to thank Tao Li and Joshua Greene for some helpful conversations. Some of this work was carried out while the authors attended the ‘‘Floer Homotopical Methods in Low Dimensional and Symplectic Topology’’ workshop at the Simons Laufer Mathematical Sciences Institute (formerly MSRI) supported by NSF Grant DMS-1928930 when the second author was in residence there during Fall 2022. Further work was carried out while the authors attended the ‘‘2022 Tech topology conference’’. We would like to thank the organisers of these two conferences. The second author was partially supported by NSF grant DMS-2104144 and a Simons Fellowship.

2. BACKGROUND AND REVIEW

In this section we review aspects of Heegaard Floer homology and $(1, 1)$ knots that will be relevant in Section 3.

2.1. Knot Floer homology and almost L-space knots. Knot Floer homology is a knot invariant due independently to Ozsváth-Szabó [OS04a] and J. Rasmussen [Ras03]. We briefly review the definition.

For a knot K , in a rational homology three sphere Y , one associates a doubly-pointed Heegaard diagram $\mathcal{H} = \{\Sigma, \alpha, \beta, z, w\}$, where Σ is a genus g surface. The symmetric product of Σ , $\text{Sym}^g(\Sigma)$, is a $2g$ -dimensional symplectic manifold obtained by taking the quotient of the g -fold Cartesian product by the natural action of the symmetric group S_g . $\text{Sym}^g(\Sigma)$ contains two Lagrangians given as the image of the following manifolds

$$\mathbb{T}_\alpha = \alpha_1 \times \cdots \times \alpha_g \quad \text{and} \quad \mathbb{T}_\beta = \beta_1 \times \cdots \times \beta_g.$$

under the quotient. Ozsváth-Szabó define a map

$$\mathfrak{s}_w: \mathbb{T}_\alpha \cap \mathbb{T}_\beta \rightarrow \text{Spin}^c(Y)$$

in [OS04b, Section 2.6]. Set $\mathfrak{T}(\mathcal{H}, s) = \{x \in \mathbb{T}_\alpha \cap \mathbb{T}_\beta \mid \mathfrak{s}_w(x) = s\}$. Suppose $[K]$ is of order d in $H_1(Y)$, then there is a function

$$A_{w,z}: \mathfrak{T}(\mathcal{H}, s) \rightarrow \frac{1}{2d}\mathbb{Z}$$

called the *Alexander grading*. See [HL19, Section 2.2], [OS11, Section 2.4]. For each $s \in \text{Spin}^c(Y)$, the knot Floer chain complex $\text{CFK}^\infty(Y, K, s)$ is generated by the tuples $[x, i, j]$ where $x \in \mathfrak{T}(\mathcal{H}, s)$, $i \in \mathbb{Z}$ and $j - i = A_{w,z}(x)$. Note that for generators in the same spin^c structure, all j are in the same

coset of \mathbb{Z} . This complex is often viewed as a free module over the polynomial ring $\mathbb{F}[U, U^{-1}]$, where $\mathbb{F} = \mathbb{Z}/2\mathbb{Z}$ and the action of U is given by $U \cdot [x, i, j] = [x, i - 1, j - 1]$. The differential is given by

$$\partial x = \sum_{y \in \mathbb{T}_\alpha \cap \mathbb{T}_\beta} \sum_{\substack{\phi \in \pi_2(x, y) \\ \mu(\phi) = 1}} \# \widehat{\mathcal{M}}(\phi) [y, i - n_w(\phi), j - n_z(\phi)],$$

where $\pi_2(x, y)$ is the set of homotopy class of Whitney disks between x and y , $\widehat{\mathcal{M}}(\phi)$ is the reduced moduli space of the holomorphic representatives of ϕ , μ is the Maslov index, and n_w (resp. n_z) is the intersection number of ϕ with a co-dimension 2 submanifold of $\text{Sym}^g(\Sigma)$ associated to the w (resp. z) basepoint. Let

$$\text{CFK}^\infty(Y, K) = \bigoplus_{s \in \text{Spin}^c(Y)} \text{CFK}^\infty(Y, K, s).$$

There is a double-filtration on $\text{CFK}^\infty(Y, K)$ induced by (i, j) . It turns out that up to doubly-filtered chain homotopy equivalence, $\text{CFK}^\infty(Y, K)$ is a topological invariant of the pair (Y, K) . Additionally, each generator is assigned an integer value called the *Maslov grading*, denoted by gr . The differential lowers the Maslov grading by 1 while the U action lowers the it by 2.

A *positive (resp. negative) L-space knot* is a knot K in an L-space Y such that sufficiently positive (resp. negative) surgeries on K yields an L-space. It turns out that those knots have particularly simple knot Floer chain complex that resembles a staircase on the (i, j) plane.

Definition 2.1. In $\text{CFK}^\infty(Y, K, s)$, a *positive staircase* is a set of generators $\{x_\ell\}_{1 \leq \ell \leq N} \cup \{y_\ell\}_{1 \leq \ell \leq N+1}$ where N is a non-negative integer, such that x_ℓ and y_ℓ only differ in i coordinate while x_ℓ and $y_{\ell+1}$ only differ in j coordinate, and the differentials are given by $\partial x_\ell = y_\ell + y_{\ell+1}$ for $1 \leq \ell \leq N$. A *negative staircase* is the dual of a positive staircase.

Suppose $K \subset Y$ is a positive (resp. negative) L-space knot. For each $s \in \text{Spin}^c(Y)$, $\text{CFK}^\infty(Y, K, s)$ consists of a positive (resp. negative) staircase. For knots in S^3 this result follows from a result of Ozsváth-Szabó [OS05, Theorem 1.2] while the general case is due to J. and S. Rasmussen [RR17, Lemma 3.2], building on work of Boileau, Boyer, Cebanu, and Walsh [BBCW12].

Next we turn to *almost L-space knots*. An *almost L-space* is a rational homology sphere Y such that $\widehat{\text{HF}}(Y, s)$ has rank 1 in all but one spin^c structure, in which it has rank 3. We call the spin^c structure in which $\text{rank}(\widehat{\text{HF}}(Y, s)) = 3$ the *exceptional spin^c structure*. A knot K in a rational homology sphere L-space is a positive (resp. negative) almost L-space knot if sufficiently positive (resp. negative) surgeries on K yield almost L-spaces and K is not a trefoil.

Definition 2.2. In $\text{CFK}^\infty(Y, K, s)$, a set of generators is called a *positive almost staircase* if for some positive integer k it is one of the following.

- (a) Generators are $\{x_\ell\}_{1 \leq \ell \leq 2k} \cup \{y_\ell\}_{1 \leq \ell \leq 2k+1} \cup \{y'_{k+1}\} \cup \{z\}$, where y_{k+1}, y'_{k+1} and z are in coordinates $(0, 1), (1, 0)$ and $(0, 0)$ respectively, x_ℓ and y_ℓ only differ in i coordinate, while x_ℓ and $y_{\ell+1}$ only differ in j coordinate except for $\ell = k$, where x_k and y'_{k+1} only differ in j coordinate. The differential is given by

$$\begin{aligned} \partial x_\ell &= y_\ell + y_{\ell+1} & 1 \leq \ell \leq 2k & \text{ and } \ell \neq k, k+1 \\ \partial x_k &= y_k + y_{k+1} + y'_{k+1} \\ \partial x_{k+1} &= y_{k+1} + y_{k+1} + y'_{k+1} \\ \partial y_{k+1} &= \partial y'_{k+1} = z; \end{aligned}$$

- (b) Generators are $\{x_\ell\}_{1 \leq \ell \leq 2k+1} \cup \{x'_{k+1}\} \cup \{y_\ell\}_{1 \leq \ell \leq 2k+2} \cup \{z\}$, where x_{k+1}, x'_{k+1} and z are at coordinate $(0, -1), (-1, 0)$ and $(0, 0)$ respectively, x_ℓ and y_ℓ only differ in i coordinate, while x_ℓ and $y_{\ell+1}$ only differ in j coordinate except for $\ell = k+1$, x'_{k+1} and y_{k+2} only differ in j coordinate. The differential has non-zero components given by

$$\begin{aligned} \partial x_\ell &= y_\ell + y_{\ell+1} & 1 \leq \ell \leq 2k+1 & \text{ and } \ell \neq k+1 \\ \partial z &= x_{k+1} + x'_{k+1} \\ \partial x_{k+1} &= \partial x'_{k+1} = y_{k+1} + y_{k+2}. \end{aligned}$$

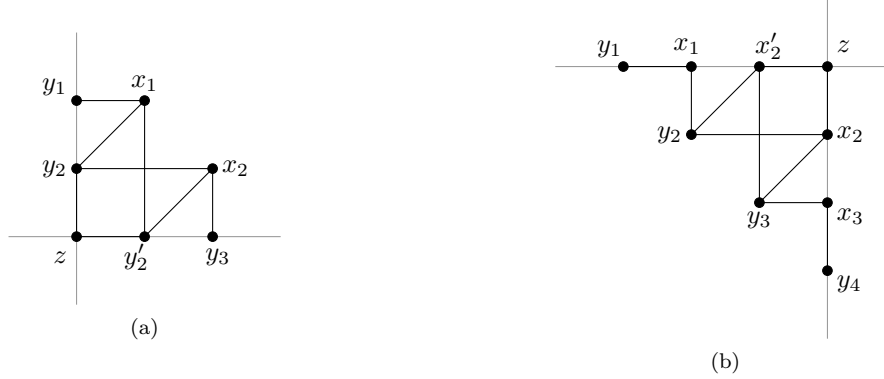


FIGURE 4. Two examples of positive almost staircases drawn in the (i, j) plane. Solid dots indicate generators and edges indicate non-trivial components of the differential (since the differential lowers the filtration level we omit the direction of the edges).

We note there are no known examples of knots with the CFK^∞ type of almost staircases of type b). A *negative almost staircase* is the dual of a positive almost staircase.

A *box with length 1* is a set of generators $\{a, b, c, d\}$ with coordinates $(0, 0)$, $(0, 1)$, $(1, 0)$ and $(1, 1)$ respectively and differential with non-trivial components given by

$$\partial d = b + c \quad \partial b = \partial c = a.$$

Theorem 2.3 ([Bin23]). *Suppose K is a positive almost L-space knot in a rational homology sphere. Then in the exceptional spin^c structure s $\text{CFK}^\infty(Y, K, s)$ consists of either*

- a direct sum of a positive staircase and a box of length 1
- or a positive almost staircase,

while in every other spin^c structure the knot Floer chain complex consists of a positive staircase.

Note that only almost L-space knots in S^3 are considered in [Bin23], but given that Ozsváth-Szabó’s large surgery formula [OS04a, Section 4] holds for rational homology spheres, the result above follows from the proof in the S^3 case, together with Ozsváth-Szabó’s classification of the CFK^∞ -type of L-space knots [OS05]. Note also that the statement holds for the negative almost L-space knot as well, replacing the word “positive” by “negative”. Finally, we note in passing that the exceptional \mathfrak{s} is necessarily self-conjugate

2.2. (1,1) knots. A $(1, 1)$ knot is a knot which can be encoded by a doubly pointed Heegaard diagram on $S^1 \times S^1$. In this setting, the definition of the knot Floer chain complex simplifies drastically. Given $\mathcal{H} = \{\Sigma, \alpha, \beta, z, w\}$, where the genus of Σ is 1, we have that $\text{Sym}^q(\Sigma) = \Sigma$, $\mathbb{T}_\alpha = \alpha$ and $\mathbb{T}_\beta = \beta$. Consider the universal cover of Σ , \mathbb{R}^2 . The orientation on Σ induces an orientation on \mathbb{R}^2 . Let $\tilde{\alpha}, \tilde{\beta}$ denote particular lifts of α and β respectively. Orienting α and β so that $\alpha \cdot \beta > 0$ induces orientations on $\tilde{\alpha}$ and $\tilde{\beta}$ so that $\tilde{\alpha} \cdot \tilde{\beta} > 0$. For $x, y \in \mathfrak{I}(\mathcal{H}) = \alpha \cap \beta$, we have $\langle \partial x, y \rangle \neq 0$ if and only if there is an embedded bigon from a lift of x to a lift of y cobounded by $\tilde{\alpha}$ and $\tilde{\beta}$ (subject to the standard orientation conditions). In sum, computing Heegaard Floer homology in the case of $(1, 1)$ knots requires no analysis.

Up to isotopy, we can ensure that each bigon in a $(1, 1)$ diagram contains at least one basepoint by successively isotoping away bigons in the complement of the basepoints, that is, by simply “pulling tight” the curves. Then by fixing a choice of the parametrization of $S^1 \times S^1$, each $(1, 1)$ diagram admits a unique *standard diagram*, encoded by a four-tuple (p, q, r, s) following the convention of J. Rasmussen [Ras05]. See Figure 1. The number p is an invariant of the knot, while q is an invariant of the diagram. A priori, s may take value in \mathbb{Z} . However, note that the transformation $(p, q, r, s) \rightarrow (p, q, r, s + p)$ amounts to performing a Dehn twist along the red α curve, which changes the isotopy class of the diagram but preserves the manifold-knot pair. Therefore for each $(1, 1)$ diagram we can choose the unique standard diagram representative such that s is in the interval $[0, p)$. There is an

involution given by reflection in the horizontal direction, which corresponds to taking the mirror of the manifold-knot pair, and corresponds to the transformation $(p, q, s, r) \rightarrow (p, q, p - 2q - r, 2q - s)$. Each $(1, 1)$ diagram is uniquely associated to a standard diagram and therefore to a four-tuple, but different standard diagrams can give rise to the same knot. We denote the $(1, 1)$ knot associated to a four-tuple (p, q, s, r) by $K(p, q, r, s)$.

Remark 2.4. In the convention of [GLV18], a $(1, 1)$ diagrams is called *reduced* if each bigon contains at least one basepoint. Note that the difference between a reduced $(1, 1)$ diagrams and a standard diagram is merely whether one fixes a parametrization of $S^1 \times S^1$ or not. Therefore one does not lose generality by making statements regarding standard diagram.

We will be interested in standard diagrams that satisfy various properties. First recall the following definition from the introduction:

Definition 1.2. ([GLV18, Definition 1.1].) A standard diagram is *coherent* if there are no inconsistent arcs.

L-space knots are diagrammatically characterized amongst $(1, 1)$ knots as follows:

Theorem 1.3. ([GLV18, Theorem 1.2].) *A standard diagram represents an L-space knot if and only if it is coherent.*

We now give a reinterpretation of Greene-Lewallen-Vafaee's proof of Theorem 1.3. This will give an indication of how we shall proceed in the case of almost L-space knots.

Fix a lift $\tilde{\alpha}$ of α in the universal cover \mathbb{R}^2 . Given $s \in \text{Spin}^c(Y)$, choose a lift of some point $x \in \mathfrak{T}(\mathcal{H}, s)$ to a point $\tilde{x} \in \tilde{\alpha}$. There is a unique lift $\tilde{\beta}_s$ of β that passes through x . The points of $\tilde{\alpha} \cap \tilde{\beta}_s$ are in one-to-one correspondence with $\mathfrak{T}(\mathcal{H}, s)$. There are $2n + 1$ such points for some non-negative integer n since $\chi(\widehat{\text{CFK}}(\mathcal{H}, s)) = 1$. Number these points $\tilde{\alpha} \cap \tilde{\beta}_s$ from 1 to $2n + 1$ according to the orientation of $\tilde{\alpha}$, with \tilde{x} as 1. Next, starting from infinity and following the orientation of $\tilde{\beta}_s$, record the sequence of the intersection points that $\tilde{\beta}_s$ passes through.

Definition 2.5. An intersection point $b \in \tilde{\alpha} \cap \tilde{\beta}_s$ is called a *turning point* if its number is either greater or less than the numbers of both its successor and predecessor in the above sequence.

The following fact is implicit in [GLV18]: a turning point admits both an incoming and an outgoing arrow in $\text{CFK}^\infty(Y, K, s)$. However, such a generator does not exist in the knot Floer chain complex of an L-space knot for any basis. We note in passing that the knot Floer chain complex of an L-space knot there is in fact a unique basis that can be obtained from a $(1, 1)$ diagram.

Lemma 2.6 ([GLV18]). *A standard diagram for an L-space knot has no turning point in the universal cover.*

In other words, the order of the sequence of the intersection points along $\tilde{\beta}_s$ is either increasing or decreasing. In each case $\tilde{\beta}_s$ is called *positive* or *negative graphic* in [GLV18]. Whether $\tilde{\beta}_s$ is positive or negative graphic depends only on whether the L-space knot is positive or negative. Therefore if this property holds for one spin^c structure it holds for all spin^c structures. It follows that the $(1, 1)$ diagram is coherent. More precisely, $\tilde{\alpha}$ separates \mathbb{R}^2 into upper and lower half planes, and in each half plane it cuts $\tilde{\beta}_s$ into n arcs and 1 ray that goes to infinity. Each rainbow arc in the $(1, 1)$ diagram around, say, the z basepoint has a lift to an arc in the lower half plane. Since the condition in Lemma 2.6 implies that the arcs in the lower half plane have the same orientation, the rainbow arcs themselves have the same orientation.

The converse of Lemma 2.6 is also true. Namely, a standard diagram that lifts to a graphic chain represents a staircase. One can prove this by using the fact that the vertical homology and the horizontal homology are both one-dimensional for $\text{CFK}^\infty(Y, K, s)$. See [GLV18, Proposition 2.6].

3. PROOF OF THE MAIN THEOREM

In this section we prove Theorem 1.5 by adapting the techniques outlined in Subsection 2.2. We also prove Proposition 1.7.

Observe that if a standard $(1, 1)$ diagram has only one rainbow arc then it is necessarily coherent, in which case it is the diagram for an L-space knot by the main result of Greene-Vafaee-Lewallen [GLV18]. We can thus restrict our attention to $(1, 1)$ diagrams which have at least two rainbow arcs.

Let $(S^1 \times S^1, \alpha, \beta, z, w)$ be a $(1, 1)$ diagram. As in the setting of L-space knots, we consider the lifts of the α and β curves to the universal cover of $S^1 \times S^1$, which is \mathbb{R}^2 . Recall that for a reduced $(1, 1)$ diagram, in the universal cover given a fixed lift $\tilde{\alpha}$, we can choose a lift $\tilde{\beta}_s$ for each $s \in \text{Spin}^c(Y)$. The curve $\tilde{\beta}_s$ is cut by $\tilde{\alpha}$ into arcs and 2 rays. Without loss of generality we may take $\tilde{\alpha}$ to be the line $\{y = 0\} \subset \mathbb{R}^2$.

Define $h(\eta)$, the *height* of an arc η as follows:

$$(2) \quad h(\eta) = \max\{|y| : (x, y) \in \eta\}.$$

We also define a notion of inconsistent arc in the universal cover \mathbb{R}^2 , that mirrors the definition in $S^1 \times S^1$. Consider the collection of curves $\{\tilde{\beta}_s : s \in \text{Spin}^c(Y)\}$. If there are two orientations amongst all the arcs in each half plane, call the direction in the minority the *inconsistent direction*, and the arcs in this direction the *inconsistent arcs*. Call the remaining arcs *consistent arcs* and their direction the *consistent direction*.

Definition 3.1. A standard diagram $(S^1 \times S^1, \alpha, \beta, z, w)$ is *virtually almost coherent* if $\bigcup_{s \in \text{Spin}^c(Y)} \tilde{\beta}_s$ contains exactly two inconsistent arcs.

Note that if there are two inconsistent arcs, there must be one in each half plane. Clearly any standard virtually almost coherent $(1, 1)$ diagram has exactly two inconsistent arcs, since each rainbow arc around z (resp. w) basepoint lifts to at least one arc in the lower (resp. upper) half plane. The converse is false, however, as illustrated by the example $K(9, 2, 0, 4)$ in Figure 5.

It turns out that virtually almost coherent is equivalent to strongly almost coherent. We recall the definition of strongly almost coherence for the reader's convenience.

Definition 1.4. A standard diagram is *strongly almost coherent* if there are exactly two inconsistent arcs and one of the following is true: ²

- the inconsistent arcs share a common end point;
- the inconsistent arcs are connected by two other rainbow arcs.

In order to show that the two versions of almost coherence are equivalent, we start with a geometric observation.

Lemma 3.2. *Suppose \mathcal{H} is a virtually almost coherent diagram. Then the height of the inconsistent arc is less than 1.*

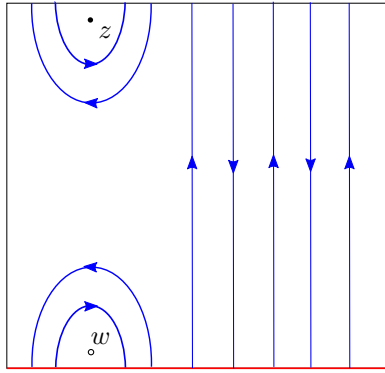
In particular, if γ is an inconsistent arc in a virtually almost coherent diagram, the bigon formed by γ and $\tilde{\alpha}$ contains exactly one basepoint.

Proof. Suppose otherwise. Then there exists an inconsistent arc γ in the upper half plane such that $h(\gamma) > 1$. Consider any bigon D formed by γ and the line $\{(x, y) \in \mathbb{R}^2 : y = \lfloor h(\gamma) \rfloor\}$. A translate of D gives another inconsistent arc of a smaller height, contradicting the virtually almost coherent condition. \square

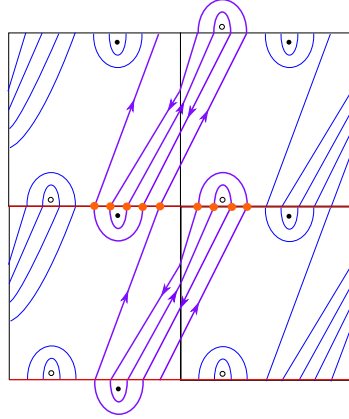
Proposition 3.3. *A standard diagram is virtually almost coherent if and only if it is strongly almost coherent.*

Proof. Let $\mathcal{H} = (\alpha, \beta, z, w)$ be a standard diagram. Suppose \mathcal{H} is virtually almost coherent. Note that by Lemma 3.2 we can assume that the inconsistent arcs are lifts of rainbow arcs. If the two inconsistent arcs in the universal cover share a common end point, the first case in Definition 1.4 applies. Suppose the two inconsistent arcs do not share an end point, then up to reflection with respect to vertical and horizontal axis, the only possible positions for the two inconsistent arcs are depicted in Figure 6 (a),(b) and (c).

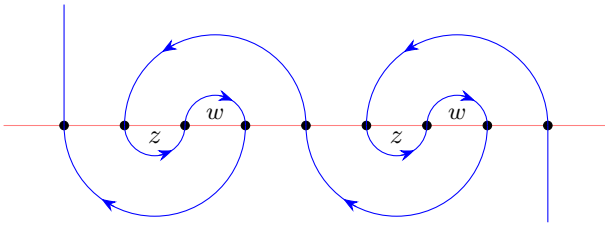
²We call a standard diagram with the same number of arcs in each direction (so that there is a choice of inconsistent direction) strongly almost coherent if for a choice of inconsistent direction one of the conditions is satisfied.



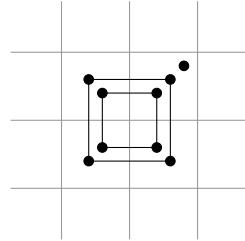
(a) The standard diagram of $K(9, 2, 0, 4)$. The i -th intersection point on the top side is identified with the $(i + 4)$ -th point on the bottom side.



(b) The lift to the universal cover of $K(9, 2, 0, 4)$. Thick solid dots indicate a choice of basis for the knot Floer complex.



(c) The lift to the universal cover.



(d) The knot Floer complex.

FIGURE 5. The knot $K(9, 2, 0, 4)$ has exactly two inconsistent arcs downstairs, but these lift to four inconsistent arcs in the universal cover. Similar examples abound amongst $(1, 1)$ knots.

We claim cases (a) and (b) do not happen. This leads to the conclusion as follows. The remaining diagram in case (c) consists of only graphic chains (view the non-compact ray as a graphic chain just for now). The bigon formed by an inconsistent arc and $\tilde{\alpha}$ admits at most one base-point. No matter which direction the inconsistent arcs go, it follows that the only possible diagram is the one depicted in Figure 6 (d), where the dashed curves indicates the remaining graphic chains. This is the second case in Definition 1.4.

To prove the claim, again notice that the remaining diagram consists of only graphic chains. Assign any direction to the inconsistent arcs, in both cases (a) and (b), the two graphic chains from the end points of either inconsistent arc either intersect each other or both go to infinity, proving the claim.

Suppose now that \mathcal{H} is strongly almost coherent, we want to show that the only inconsistent arcs in the universal cover are the ones with height less than 1, in other words, the lift of the two inconsistent rainbow arcs. Consider any other arc and the bigon D it forms with $\tilde{\alpha}$. Any inconsistent sub-arcs on ∂D appears in one of the two local models in Definition 1.4; observe that such local inconsistency also necessarily occurs on $\tilde{\alpha}' : \{y = c\}$ for some $c \neq 0$. Replacing the entire sub-arc of $\tilde{\beta}$ in the local model by the sub-arc of $\tilde{\alpha}'$ with the same end points preserves the orientation of ∂D . After performing this operation on every local inconsistency on ∂D , the only local maximum or minimum are of consistent orientation. It follows that ∂D is consistently oriented. \square

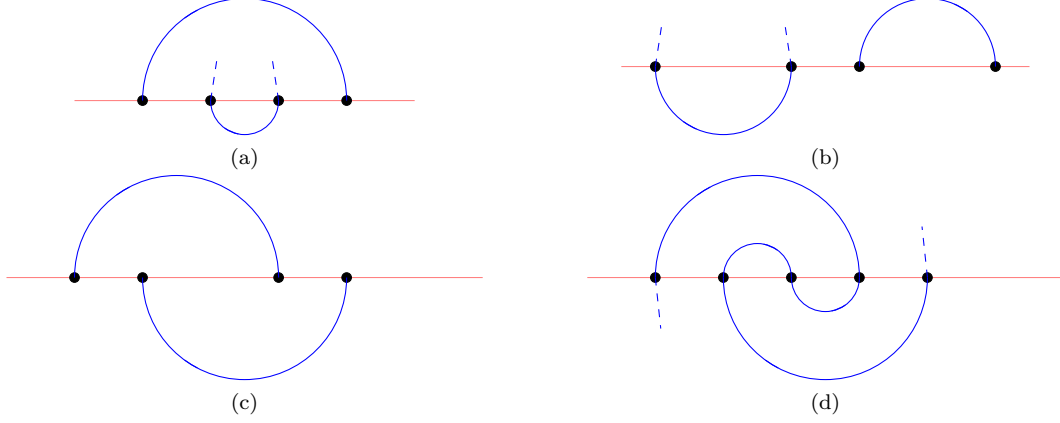


FIGURE 6. Up to reflection with respect to vertical and horizontal axis, the only possible positions for the two inconsistent arcs are Figure (a) (b) and (c).

Thus to prove Theorem 1.5 it suffices to prove the following.

Theorem 3.4. *A standard diagram represents an almost L-space knot if and only if it is virtually almost coherent. Moreover, if $K \subset Y$ is a $(1, 1)$ almost L-space knot and s is the exceptional spin^c structure, then $\text{CFK}^\infty(Y, K, s)$ consists of the direct sum of a staircase and a box of length one.*

We will prove both directions of this theorem individually in Proposition 3.10 and 3.12. First we show that if K is a $(1, 1)$ almost L-space knot then any standard diagram for K is virtually almost coherent.

Up to translation by U as a whole, $\mathfrak{T}(\mathcal{H}, s) = \tilde{\alpha} \cap \tilde{\beta}_s$ gives rise to a specific basis of $\text{CFK}^\infty(Y, K, s)$ as follows. Choose any $x \in \mathfrak{T}(\mathcal{H}, s)$, starting from $[x, 0, A_{w,z}(x)]$, for any $y \in \mathfrak{T}(\mathcal{H}, s)$ with a bigon connected to x , add $[y, i, j]$ into the basis where $[x, 0, A_{w,z}(x)] \in \partial[y, i, j]$ or $[y, i, j] \in \partial[x, 0, A_{w,z}(x)]$. Continue this process until exhausting $\mathfrak{T}(\mathcal{H}, s)$. The resulting basis is connected by components of the differential of the chain complex. Abusing notation we let $\mathfrak{T}(\mathcal{H}, s)$ also denote this specific basis for $\text{CFK}^\infty(Y, K, s)$.

Throughout the remainder of this section we let K be an almost L-space knot in a rational homology sphere Y with exceptional spin^c structure s .

Lemma 3.5. *Let \mathcal{H} be a standard diagram representing an almost L-space knot. The generators in the basis $\mathfrak{T}(\mathcal{H}, s)$ are in either 3 or 4 consecutive Maslov gradings. Moreover, the number of the generators in each Maslov grading (from high to low) is given by one of the following ;*

- (a) $(1, *, *)$,
- (b) $(*, *, 1)$,
- (c) $(1, 2, *, *)$,
- (d) $(*, *, 2, 1)$,

where each $*$ indicates some (potentially different) positive integer.

Proof. According to Theorem 2.3, up to filtered change of basis, $\text{CFK}^\infty(Y, K, s)$ is either a summand of a staircase and a length 1 box or an almost staircase.

Start with the first case. Suppose that after a filtered change of basis, $\mathfrak{T}(\mathcal{H}, s)$ becomes the set $\mathfrak{S}_1 \cup \mathfrak{S}_2$ where \mathfrak{S}_1 generates the staircase summand and \mathfrak{S}_2 generates the box summand. We know that generators in $\mathfrak{T}(\mathcal{H}, s)$ initially are connected by differentials, therefore the Maslov gradings of \mathfrak{S}_1 and \mathfrak{S}_2 can coincide in either 1 or 2 consecutive gradings. (This follows because one must be able to add elements from \mathfrak{S}_1 and \mathfrak{S}_2 homogeneously in order to return to $\mathfrak{T}(\mathcal{H}, s)$.) The property that a basis satisfies the condition given in the lemma is preserved by filtered change of basis. Thus one simply checks that the lemma holds for the standard basis for a staircase plus a box given the suitable Maslov grading.

Suppose that after a filtered change of basis $\mathfrak{T}(\mathcal{H}, s)$ generates an almost staircase complex. Then again one simply checks that the lemma holds for the standard basis of an almost staircase in Definition 2.2. \square

We now refine the definition of the turning points given in Subsection 2.2. Note that by definition, a turning point necessarily has a predecessor and a successor (along $\tilde{\beta}_s$, following its orientation).

Definition 3.6. Suppose b is a turning point and a its predecessor. If $a \in \partial b$, we call b a *positive* turning point and if $b \in \partial a$, we call b a *negative* turning point.

Note that each turning point together with its predecessor and successor live in 3 consecutive Maslov gradings. The order in which $\tilde{\beta}_s$ passes through them depends on the sign of the turning point at b .

Lemma 3.7. *Moving along $\tilde{\beta}_s$, suppose b and c (in that order) are two closest turning points. Consider the set of the points in $\tilde{\alpha} \cap \tilde{\beta}_s$ between b and c along $\tilde{\beta}_s$ (including the end points) and label them in order by $x_0 = b, x_1, \dots, x_\ell, \dots$. Their Maslov gradings satisfy*

$$\text{gr}(x_\ell) = \begin{cases} \text{gr}(b) & \ell \text{ is even} \\ \text{gr}(b) + 1 & \ell \text{ is odd and } b \text{ is a positive turning point} \\ \text{gr}(b) - 1 & \ell \text{ is odd and } b \text{ is a negative turning point.} \end{cases}$$

Proof. Suppose that b is a positive turning point. Then we have

$$\partial x_\ell = x_{\ell+1} + x_{\ell-1}$$

for each odd ℓ . If b is a negative turning, then we have

$$\partial x_{\ell+1} = \partial x_{\ell-1} = x_\ell$$

for each odd ℓ . The Maslov grading results follow. \square

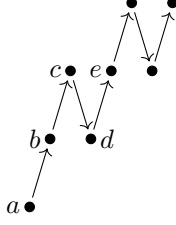
Lemma 3.8. *Let \mathcal{H} be a standard diagram representing an almost L-space knot. The unique generator in $\mathfrak{T}(\mathcal{H}, s)$ with the highest/lowest Maslov grading has both a predecessor and a successor along $\tilde{\beta}_s$.*

Proof. Up to reflecting \mathbb{R}^2 about $\tilde{\alpha}$ (recall that the mirror of an almost L-space knot is also an almost L-space knot), we may assume that the number of generators in each Maslov grading is either $(*, *, 1)$ or $(*, *, 2, 1)$. Let a be the unique generator with the lowest Maslov grading. Assume towards a contradiction that a has no predecessor. Then a has a successor b , and b is necessarily a turning point; let c be the successor of b .

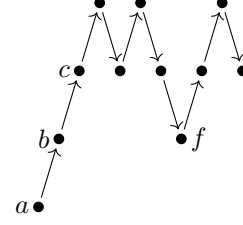
- Case of $(*, *, 1)$. There is no turning points after b , so all the remaining generators lie between a and c on $\tilde{\alpha}$ (and in particular, between a and b). This contradicts the fact the ray in the positive direction of $\tilde{\beta}_s$ lies outside of the bigon between a and b .
- Case of $(*, *, 2, 1)$. Due to the Maslov grading, there are three possibilities:
 - 1.) c is a turning point;
 - 2.) c is not a turning point. The successor of c , denoted by d , is a turning point;
 - 3.) neither c nor d are turning points. The successor of d , denoted by e , is a turning point.

Case 2.): the successor of d would be in the same Maslov grading as a , a contradiction.
Case 3.): note that b and d are the only generators in the second lowest Maslov grading. It follows that there is no more turning after e . But again in this case the remaining generators lie between a and b on $\tilde{\alpha}$, contradicting the fact that the ray in the positive direction of $\tilde{\beta}_s$ lies outside of the bigon between a and b .
Case 1.): since the ray in the positive direction of $\tilde{\beta}_s$ lies outside of the bigon between a and b , there has to be a turning after c , which has to be a negative turning due to the Maslov grading; let f be the successor of this turning point. Observe that f is between a and b , and the only generators in the second lowest Maslov grading are b and f . Therefore the argument in Case 3.) applies, leading to a contradiction.

\square



(a) Case 2.) in the proof of Lemma 3.8.



(b) Case 3.) in the proof of Lemma 3.8.

FIGURE 7. The height indicates the Maslov grading, and the arrow indicates the direction of $\tilde{\beta}_s$. Note that a point is a turning point if and only if it is between two consecutive arrows of the same direction, and it is a positive (resp. negative) turning if both arrows point upwards (resp. downwards).

We often find it helpful to record diagrammatically the Maslov grading and the direction of $\tilde{\beta}_s$. See Figure 7(a) and 7(b) for the corresponding diagram of case 2.) and case 3.) in the above proof respectively.

Definition 3.9. Let b, \dots, c be a series of points along $\tilde{\beta}_s$ in that order. Suppose that either

- b has no predecessor,
- or d has no successor,
- or a is the predecessor of b , d is the successor of c , and $(\tilde{\alpha} \cdot \tilde{\beta}_s)|_a \cdot (\tilde{\alpha} \cdot \tilde{\beta}_s)|_d > 0$.

Assume furthermore that there are no turning points in $\tilde{\alpha} \cap \tilde{\beta}_s \setminus \{a, b, \dots, c, d\}$. Consider the following operation: first remove $\{b, \dots, c\}$ and all the arcs connecting to them; then identify a and d (if they exist). We call this operation *truncating the portion between b and c* . Note that the resulting $\tilde{\beta}'_s$ has no turning point, and therefore is graphic.

Proposition 3.10. *If a standard diagram represents an almost L-space knot, then it is virtually almost coherent.*

Proof. Let s be the exceptional spin^c structure. Up to reflecting \mathbb{R}^2 , we may assume the number of generators in $\mathfrak{X}(\mathcal{H}, s)$ in each Maslov grading is either $(*, *, 1)$ or $(*, *, 2, 1)$. In both cases, let a be the unique generator in the lowest Maslov grading. According to Lemma 3.8, a has a predecessor b and a successor c . If b has a predecessor, then b is a turning point, and likewise for c . There are no turning points in $\tilde{\alpha} \cap \tilde{\beta}_s \setminus \{b, c, \text{the predecessor of } b, \text{the successor of } c\}$ due to Maslov grading. Truncating the portion between b and c , we obtain a graphic chain, corresponding to a staircase. Moreover, the sign of the staircase only depends on whether the almost L-space knot is positive or negative, and therefore is uniform across all spin^c structures. The truncated portion can have at most 1 arc in each direction in each half plane. It follows that the diagram is virtually almost coherent. \square

We now prove the converse to Proposition 3.10. As claimed earlier, we will prove a stronger version of the converse: that all $(1, 1)$ almost L-space knots have the CFK^∞ -type of complexes consisting of a staircase and a box of length 1. Before the proof, we rule out a corner case. The following lemma rules out the possibility that for a virtually almost coherent $(1, 1)$ diagram, $\text{CFK}^\infty(Y, K, s)$ contains a single staircase (with varying signs) in each $s \in \text{Spin}^c(Y)$. It turns out that Definition 3.1 implies that in the exceptional spin^c structure, $\tilde{\beta}_s$ contains at least two arcs in each half plane, one of them being the inconsistent arc.

Lemma 3.11. *For a virtually almost coherent $(1, 1)$ diagram, suppose $\tilde{\beta}_s$ contains the inconsistent arcs. Then $\tilde{\beta}_s$ contains at least two arcs in each half plane.*

Proof. Assume towards the contradiction that $\tilde{\alpha}$ cuts $\tilde{\beta}_s$ into one arc and one ray in each half plane. Without loss of generality, we may assume $\tilde{\beta}_s$ starts from the lower half plane and the graphic chain goes from left to right. According to the definition, $\tilde{\beta}_s$ intersects some other lift of α in another graphic

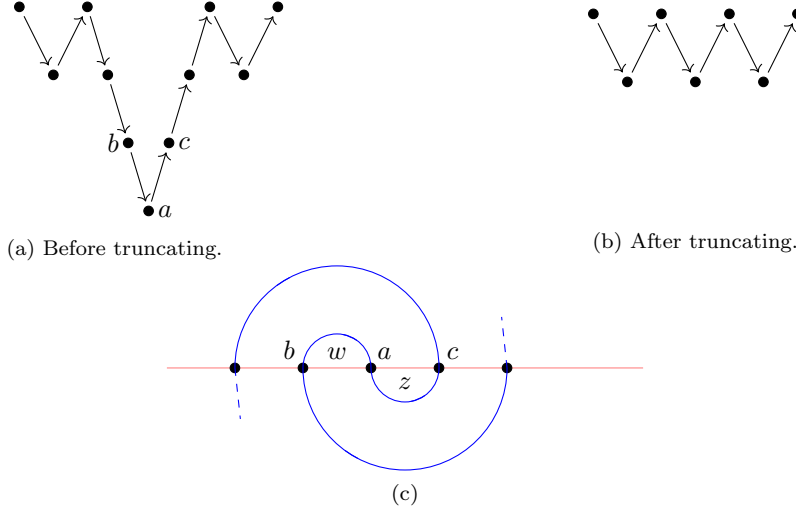


FIGURE 8. Figure (a) and (b) show the Maslov diagram before and after truncating the portion between b and c in the case of $(*, *, 2, 1)$ in the proof of Proposition 3.10. Up to reflecting \mathbb{R}^2 about $\tilde{\alpha}$, Figure (c) depicts the only possibility for the truncated portion in the above case.

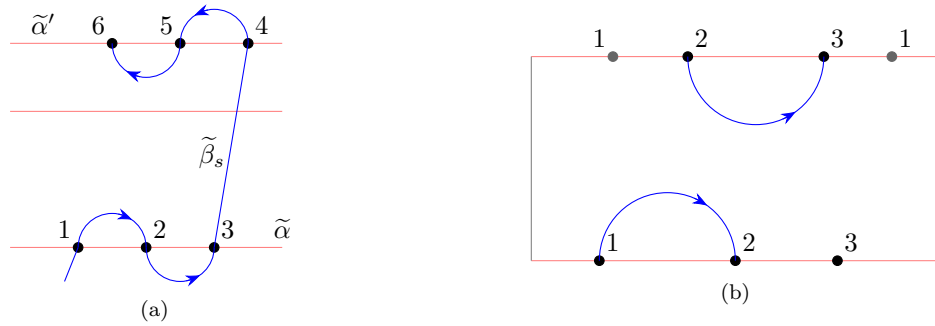


FIGURE 9. The universal cover depicted in Figure (a) cannot be a lift of any reduced $(1, 1)$ diagram. Figure (b) is a schematic picture of the standard $(1, 1)$ diagram that corresponds to Figure (a), with the possible locations of the intersection point 1 depicted. The intersection points 4 and 5 are next to 1 and 2 on the bottom side.

chain (with the opposite direction). Let $\tilde{\alpha}'$ be the first such a lift after $\tilde{\alpha}$. Name the intersection points that $\tilde{\beta}_s$ passes through by positive integers in order. See Figure 9 (a).

Project the intersection points to the standard $(1, 1)$ diagram. Note that since the top and bottom side of the standard $(1, 1)$ diagram are identified by a shift, the cyclic order of the numbering (say) from left to right is invariant on each side. The cyclic order of the first three intersection points is $(1, 2, 3)$ on both top and bottom side. Now consider 4 and 5 on the bottom side. Since they are end points of a rainbow arc, the possible cyclic order are $(1, 5, 4, 2, 3)$ or $(5, 1, 2, 4, 3)$. However, $(1, 5, 4, 2, 3)$ cannot be a cyclic order on the top side, since 5 is between 1 and 4, but 5 is an end point of a rainbow arc while both 1 and 4 are not. Similarly $(5, 1, 2, 4, 3)$ also cannot be a cyclic order on the top side, since 4 is between 2 and 3, which are two end points of a rainbow arc while 4 is not an end point of any rainbow arc. We have arrived at a contradiction. \square

Proposition 3.12. *Virtually almost coherent diagrams represent almost L -space knots. Moreover, for such knots, the knot Floer complex in the exceptional spin^c structure consists of a staircase direct summed with a box with length 1.*

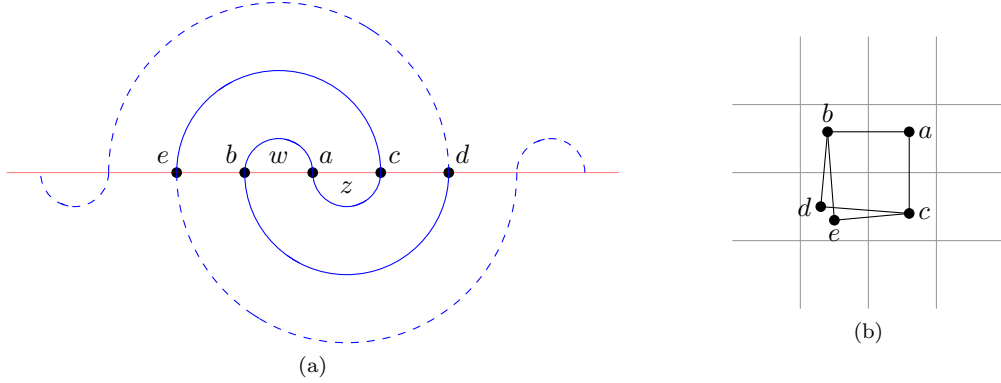


FIGURE 10. The case when the two distinct arcs do not share a common end point.

Proof. Let γ and η be the two inconsistent arcs in the lower and upper planes, respectively. There are two cases depending on whether γ and η share a common end point or not.

First consider the case in which γ and η have no common end point. Let $\partial\gamma = \{b, d\}$ and $\partial\eta = \{c, e\}$. Observe that one of the end points of γ is between c and e ; let it be b . Without loss of generality, we may assume that d is to the right of b and c is to the right of e . This is depicted in Figure 10 (a). Note that the remainder of the diagram is graphic to the right of e and to the left of d . Moreover, the predecessor/successor of d (the one other than b) must be outside the interval $[e, d]$ on $\tilde{\alpha}$, because otherwise there will be at least 2 basepoints in the bigon formed by γ and $\tilde{\alpha}$. The corresponding statement holds for e . Thus the differentials in the diagram satisfy

$$\begin{aligned}\partial a &= b + c \\ \partial b &= \partial c = e + d \\ \partial(e + d) &= 0\end{aligned}$$

The subcomplex D generated by $\{a, b, c, d+e\}$ is a box with length 1. Truncating $\{a, b, c\}$ (as defined in Definition 3.9) corresponds to quotienting D from $\text{CFK}^\infty(Y, K, s)$. Since the result of the truncation is graphic, the same argument given in the proof of [GLV18, Proposition 2.6], shows that the remaining portion of $\text{CFK}^\infty(Y, K, s)$ is a staircase complex. Therefore $\text{CFK}^\infty(Y, K, s)$ is the direct sum of a staircase and a box with length 1 as required.

Now suppose γ and η share a common end point. Let $\partial\gamma = \{a, c\}$ and $\partial\eta = \{a, b\}$. Without loss of generality, we may assume that c is to the right of b . We may also assume without loss of generality that $\tilde{\beta}_s$ is oriented such that it passes through c, a and b in that order; the same argument holds for the other orientation. Let d be the successor of b , and e the predecessor of c . There are three subcases depending on whether d and e are in the interval $[b, c]$ on $\tilde{\alpha}$.

- Suppose both d and e are in the interval $[b, c]$. Note that in this case d has a successor f and e has a predecessor g , as depicted in Figure 11 (a). The remaining diagram is graphic to the right of f and to the left of g . Moreover, suppose f has a successor, then it is necessarily outside the interval $[b, c]$. In particular, this implies the differentials in the diagram satisfy

$$\begin{aligned}\partial a &= b + c + g + f \\ \partial(b + g) &= \partial(c + f) = e + d.\end{aligned}$$

The subcomplex D generated by $\{a, b + g, c + f, d + e\}$ is a box with length 1. Truncating $\{a, b, c\}$ corresponds to quotienting D from $\text{CFK}^\infty(Y, K, s)$, and the result is a staircase.

- Suppose both d and e are outside the interval $[b, c]$. This is depicted in Figure 11 (c). Note that the remaining diagram is graphic to the right of d and to the left of e . The differentials in the diagram are

$$\begin{aligned}\partial a &= b + c \\ \partial b &= \partial c = e + d.\end{aligned}$$

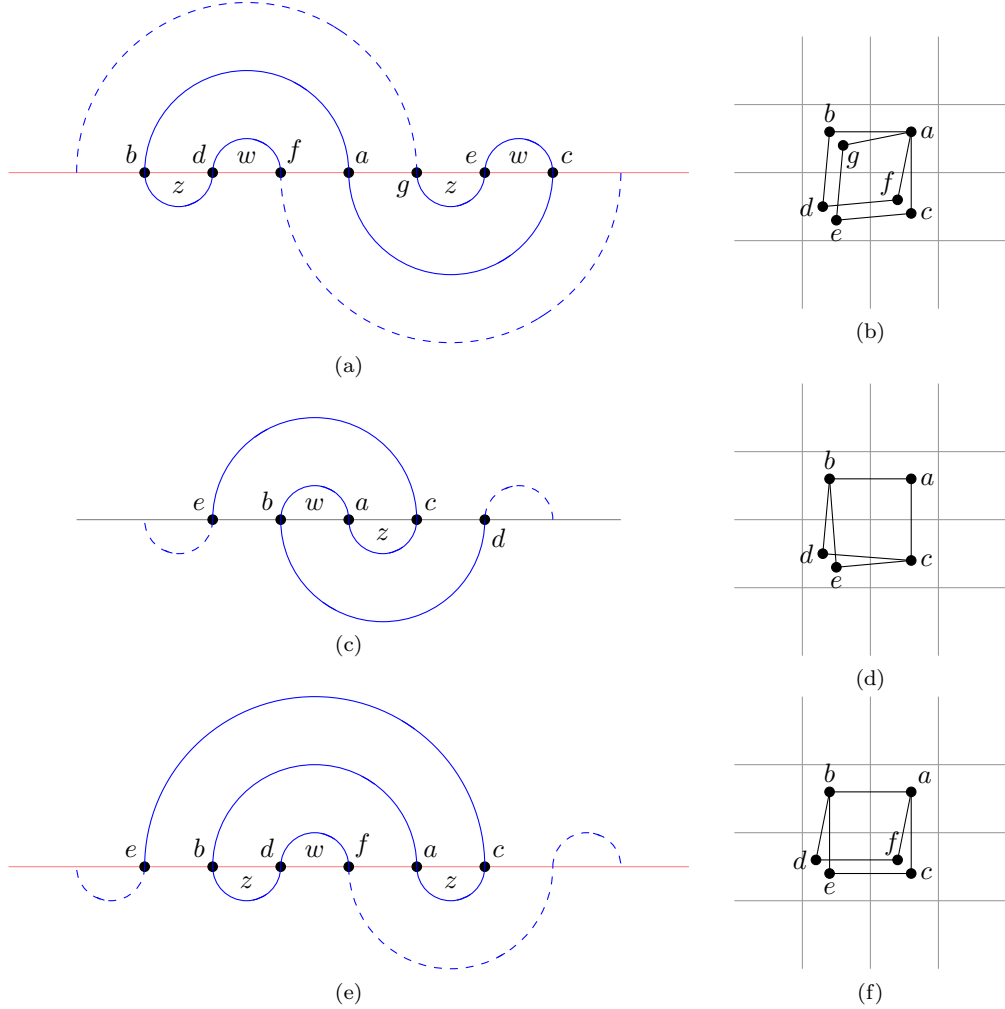


FIGURE 11. The cases when the two distinct arcs share a common end point.

The subcomplex D generated by $\{a, b, c, d + e\}$ is a box with length 1. Truncating $\{a, b, c\}$ corresponds to quotienting D from $\text{CFK}^\infty(Y, K, s)$, and the result is a staircase.

- Finally suppose d is in the interval $[b, c]$ while e is outside. The other case will follow in parallel. As depicted in Figure 11 (e), in this case we have that d has a successor f . The differentials in the diagram are

$$\begin{aligned} \partial a &= b + f + c \\ \partial b &= d + e \\ \partial c &= e \\ \partial f &= d. \end{aligned}$$

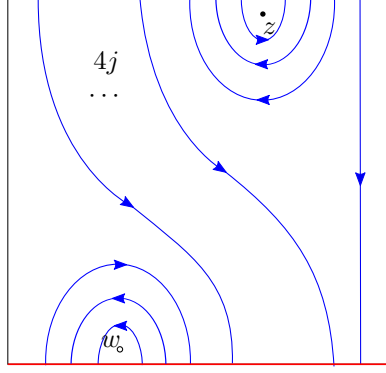
The subcomplex D generated by $\{a, b, f + c, d + e\}$ is a box with length 1. Truncating $\{a, b, c\}$ corresponds to quotienting D from $\text{CFK}^\infty(Y, K, s)$, and the result is a staircase.

□

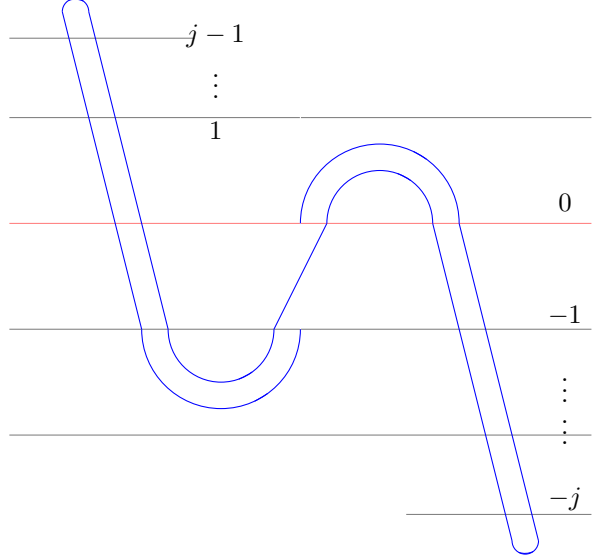
We conclude this paper by proving our result on homology cobordism:

Proposition 1.7. *The family $\{K_j\}_{j \geq 0}$ satisfies the following properties.*

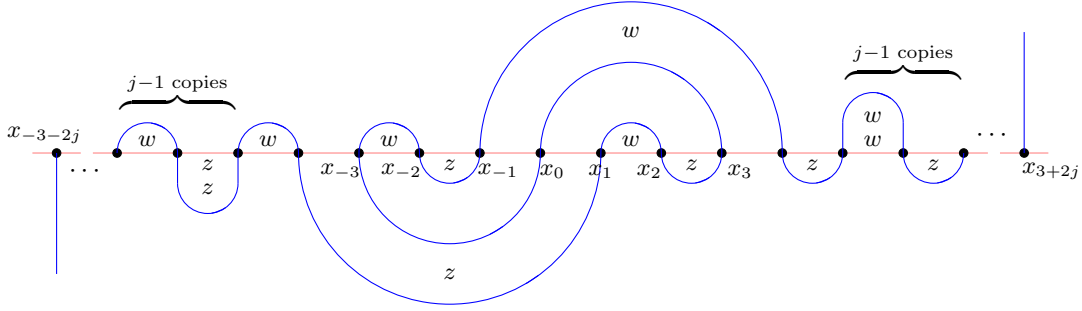
- (1) *The family $\{(S_{+1}^3(K_j) \# -S_{+1}^3(K_j), \mu \# U)\}_{j > 0}$ generates a \mathbb{Z}^∞ summand in $\widehat{\mathcal{C}}_{\mathbb{Z}}/\mathcal{C}_{\mathbb{Z}}$, where μ is the image of a meridian of K_j and U is the unknot;*



(a) The standard diagram of K_j . The i -th intersection point on the top side is identified with the $(i + 2)$ -th point on the bottom side.



(b) One iteration of the β curve in the universal cover.



(c) The lift to the universal cover, when $j \geq 1$.

FIGURE 12. Each knot $K_j = K(7+4j, 3, 4j, 2)$ for $j \geq 0$ is strongly almost coherent.

(2) K_j is not homology concordant to any L -space knot.

The argument we use for claim (2) is well-known to experts in involutive knot Floer homology, and we write it down here for the sake of completeness.

Proof of Proposition 1.7. The lift to the universal cover is obtained by concatenate $2j$ iterations of the portion displayed in Figure 12(b) and then pull tight the curve. Choose a basis x_i with $|j| \leq 3+2j$ as shown in Figure 12(c), where x_0 is the middle intersection point. When $j \geq 1$, the differential is given by

$$\begin{aligned} \partial x_{\pm 2} &= x_{\pm 3} + x_{\pm 1} \\ \partial x_{\pm 3} &= \partial x_{\pm 1} = x_0 \\ \partial x_{\pm 4} &= x_{\pm 5} + x_{\pm 3} + x_{\pm 1} \\ \partial x_{\pm 2i} &= x_{\pm 2i+1} + x_{\pm 2i-1} \quad \text{for } 3 \leq i \leq j+1. \end{aligned}$$

After a filtered change of basis

$$\begin{aligned} y_0 &= x_2 + x_{-2} \\ y_1 &= x_3 + x_{-1} \\ y_{-1} &= x_{-3} + x_1 \\ y_{\pm i} &= x_{\pm(i+2)} \quad \text{for } 2 \leq i \leq 2j, \end{aligned}$$

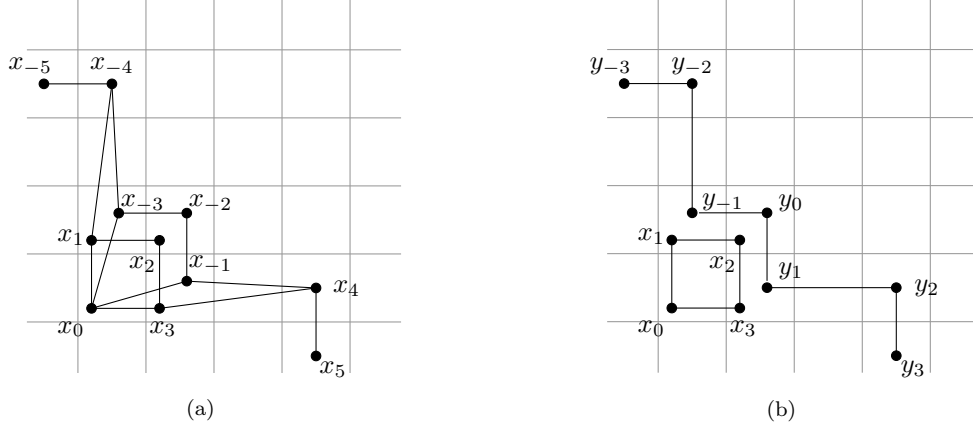


FIGURE 13. The knot Floer complex of K_1 , before and after change of basis.

we obtain a direct summand of a positive staircase D_j generated by $\{y_i \mid -2j - 1 \leq i \leq 2j + 1\}$ and a box generated by $\{x_0, x_1, x_2, x_3\}$.

Quotienting out the box complex induces a local equivalence. The remaining staircase D_j has $3+4j$ generators, with total horizontal length of the top half of the staircase $n(D_j) = j + 1$. Therefore we can apply [Zho21, Theorem 3.1] (See also [Zho21, Remark 3.3]). Finally [DHST21, Theorem 1.1] applies and we obtain a surjective homomorphism $\bigoplus_{j>0} \varphi_{j+1,j} : \widehat{\mathcal{C}}_{\mathbb{Z}}/\mathcal{C}_{\mathbb{Z}} \rightarrow \bigoplus_{j>0} \mathbb{Z}$. In particular we have $\varphi_{j+1,j}(S_{+1}^3(K_j), \mu) \neq 0$ for $j > 0$. This proves claim (1).

We prove claim (2) by considering the Hendricks-Manolescu's involution ι on $\text{CFK}^\infty(K_j)$. Since ι is a skew-filtered, grading-preserving chain map that squares to the Sarkar map, up to filtered homotopy equivalent one may take ι to send $y_0 \mapsto y_0 + U^{-1}x_0$ and $x_2 \mapsto x_2 + y_0$, and to be reflection about the line $i = j$ for every other element. (This is essentially the same computation as those in [HM17, Section 8].)

Assume to the contradiction that K_j is concordant to an L-space knot. Then as an ι_K -complex ([Zem19, Definition 2.2]), $(\text{CFK}^\infty(K_j), \iota)$ is locally equivalent to (D, ι') , where D is a staircase and ι' is the canonical involution. In fact, D must be isomorphic D_j , the staircase complex generated by all y_i . Let $f : (\text{CFK}^\infty(K_j), \iota) \rightarrow (D_j, \iota')$ be an ι_K -local map. As a graded, filtered map f sends each y_i to itself and either $x_2 \mapsto 0$ or $x_2 \mapsto y_0$. In either case, we have

$$H\partial(x_2) + \partial H(x_2) = f\iota(x_2) + \iota'f(x_2) = f(x_2 + y_0) + \iota'f(x_2) = y_0$$

for some map H . It follows that $H(x_1 + x_3) + y_0 \in \text{im } \partial$. On the other hand, we have $f(x_1 + x_3) = f\partial(x_2) = \partial f(x_2) = 0$ or $y_1 + y_{-1}$. In either case, we compute

$$0 = f\iota(x_1 + x_3) + \iota'f(x_1 + x_3) = H\partial(x_1 + x_3) + \partial H(x_1 + x_3) = y_1 + y_{-1},$$

a contradiction. It follows that K_j is not concordant to any L-space knot. \square

4. ADDENDUM

In this section we provide the code used to obtain the list of four-tuples encoding $(1, 1)$ almost L-space knots listed in Table 1. One can write a code that checks the strongly almost coherent condition quite easily, but in practice, we find an algorithm that counts inconsistent arcs in the universal cover more illuminating, and potentially more useful in more general settings. Therefore we provide an algorithm which achieves the latter.

Given a standard $(1, 1)$ diagram associated to (p, q, r, s) , to each intersection point x in the rectangle in Figure 1 we can assign a three-tuple $[position, direction, side]$, such that each intersection point of $\alpha \cap \beta$ in $S^1 \times S^1$ has a one-to-two mapping to the three-tuples. Here *position* takes integer value, recording position data in the universal cover, such that $(position \bmod p)$ specifies the position of x on a given side of the rectangle; *direction* takes value in ± 1 , recording the direction in which the β

curve intersects α at x , where 1 indicates upwards and -1 indicates downwards; $side$ takes value in ± 1 , where 1 indicates the top side of the rectangle and -1 the bottom side.

When viewing intersection points in the universal cover \mathbb{R}^2 (where $S^1 \times S^1$ gives a $\mathbb{Z} \times \mathbb{Z}$ lattice), we can assign one more parameter: $height$, which takes integer value, indicating that (a given lift of) the intersection point x lives in the line $\{y = height\}$.

The strategy of the algorithm is: we follow a lift $\tilde{\beta}$ of β in the universal cover and record the four-tuples $[position, direction, side, height]$ of intersection points in order. This encodes all the information of the lifted curves. Since $\tilde{\beta}$ is cut by $\tilde{\alpha}$ into arcs and two rays, we then simply count the number of arcs of each direction in upper half plane.

In particular, Algorithm 1 gives a function that produces the next four-tuple in the sequence. Using this function, we first obtain a sequence that encodes a portion of the curve $\tilde{\beta}$ in \mathbb{R}^2 that corresponds to one iteration of the curve β downstairs. In order to include all intersection points on the chosen lift $\tilde{\alpha}$, i.e. the line $\{y = 0\}$, we have to decide how many iterations one needs to go through. This is done in the first half of Algorithm 2.

Algorithm 1:

```

Data:  $(p, q, r, s)$ 
Result: A function that with input of the current four-tuple  $[position, direction, side, height]$ ,
           outputs the next four-tuple in the sequence. This is used to determine a path of
           intersection points that  $\tilde{\beta}$  travels through in order.
def FindNext( $[position, direction, side, height]$ ):
    // Define a function FindNext. Input: current four-tuple; Output: next four-tuple.
    if  $side = 1$  and  $direction = 1$  then
        return  $[position + s, direction, -1, height]$ 
    if  $side = -1$  and  $direction = -1$  then
        return  $[position - s, direction, 1, height]$  // Identify two sides of the rectangle

    if  $side = 1$  and  $direction = -1$  // Suppose starting from the top side of the rectangle
    then
        if  $position \% p \leq r - 1$  // For the first  $r$  strands
        then
            return  $[position + 2 * q, direction, -1, height - 1]$ 
        if  $r \leq position \% p \leq r + 2 * q - 1$  // For the rainbow arcs
        then
            return  $[2 * r + 2 * q - 1 - 2 * position \% p + position, 1, 1, height]$ 
        else
            return  $[position, direction, -1, height - 1]$  // For the remaining strands
    else
        // Suppose starting from the bottom side of the rectangle
        if  $position \% p \leq 2 * q - 1$  // For the rainbow arcs
        then
            return  $[2 * q - 1 - 2 * position \% p + position, -1, -1, height]$ 
        if  $2 * q \leq position \% p \leq r + 2 * q - 1$  // For the next  $r$  strands
        then
            return  $[position - 2 * q, direction, 1, height + 1]$ 
        else
            return  $[position, direction, 1, height + 1]$  // For the remaining strands

```

Algorithm 2:

Data: Continue from Algorithm 1.

Result: Number of inconsistent arcs in the upper half plane of the universal cover.

```
begin
  Set  $initial\_sequence = [[0, 1, 1, 0]]$  // Let the starting point be  $[0, 1, 1, 0]$ 

  while  $[position, side] \neq [0, 1]$  // Until  $\beta$  returns to the original position downstairs
  do
     $initial\_sequence.append(\text{FindNext}([position, direction, side, height]))$  // Keep adding the
    next four-tuple to the string

  Set  $max\_height = \max\{initial\_sequence.height\}$  // The maximal height

  Set  $min\_height = \min\{initial\_sequence.height\}$  // The minimal height

  Set
   $\Delta_{height} = initial\_sequence[\text{length}(initial\_sequence) - 1].height - initial\_sequence[0].height$ 
  // The height difference from the beginning to ending position

  /* Depending on the sign of  $\Delta_{height}$ , we will decide number of iterations needed to exhaust
  all the intersection points on a chosen lift of  $\alpha$ . */
  Set  $full\_sequence = initial\_sequence$ 
  if  $\Delta_{height} < 0$  then
     $iteration = \lceil \frac{min\_height - max\_height}{\Delta_{height}} \rceil$ 
  else
    if  $\Delta_{height} > 0$  then
       $iteration = \lceil \frac{max\_height - min\_height}{\Delta_{height}} \rceil$ 
    else
       $iteration = 0$ 

  while  $\text{length}(full\_sequence) \leq (iteration + 1) * (\text{length}(initial\_sequence) - 1)$  do
     $full\_sequence.append(\text{FindNext}([position, direction, side, height]))$ 
  /* For simplicity, next let us only consider when  $\Delta_{height} \geq 0$ . The other case is similar. */
  For each element of  $full\_sequence$ , set  $height = height - max\_height$ 
  // Adjust height such that  $\{y = 0\}$  is in the middle. We now have the entire portion of  $\tilde{\beta}$ 
  that includes all intersection points of  $\tilde{\beta} \cap \tilde{\alpha}$ .
  Set  $[positive, negative] = [0, 0]$ 
  Create a sub-sequence of  $full\_sequence$  with  $[side, height] = [-1, 0]$ ; call it  $intersect$ .
  /* Recall that  $\tilde{\alpha}$  cuts  $\tilde{\beta}$  into arcs and two rays. We only consider the upper half plane.
  Note that the condition  $\Delta_{height} \geq 0$  guarantees that the ray in the upper half plane meets
   $\{y = 0\}$  at the last intersection point in the subsequent  $intersect$ . */
  For  $0 \leq i \leq \lfloor \frac{\text{length}(intersect)}{2} \rfloor$ 
  if  $intersect[2i].position < intersect[2i + 1].position$  // The  $(2i + 1)$ -th and the  $(2i + 2)$ -th
  points in the sequence  $intersect$  are connected by an arc.
  then
     $positive = positive + 1$ 
  else
     $negative = negative + 1$ 
  return  $\min\{positive, negative\}$ 
```

REFERENCES

- [BBCW12] Michel Boileau, Steven Boyer, Radu Cebanu, and Genevieve S Walsh, *Knot commensurability and the berger conjecture*, *Geometry & Topology* **16** (2012), no. 2, 625–664.
- [Bin23] Fraser Binns, *The CFK^∞ type of almost L -space knots*, arXiv preprint arXiv:2303.07249 (2023).
- [BS22] John A Baldwin and Steven Sivek, *Characterizing slopes for 5_2*, arXiv preprint arXiv:2209.09805 (2022).
- [DHST21] Irving Dai, Jennifer Hom, Matthew Stoffregen, and Linh Truong, *Homology concordance and knot floer homology*, arXiv preprint arXiv:2110.14803 (2021).
- [Doy05] Gabriel Doyle, *Calculating the knot floer homology of $(1, 1)$ knots*.
- [Fuj96] Hirozumi Fujii, *Geometric indices and the alexander polynomial of a knot*, *Proceedings of the American Mathematical Society* **124** (1996), no. 9, 2923–2933.
- [GLV18] Joshua Evan Greene, Sam Lewallen, and Faramarz Vafaee, *$(1, 1)$ L -space knots*, *Compos. Math.* **154** (2018), no. 5, 918–933. MR 3798589
- [GMM05] Hiroshi Goda, Hiroshi Matsuda, and Takayuki Morifuji, *Knot floer homology of $(1, 1)$ -knots*, *Geometriae Dedicata* **112** (2005), no. 1, 197–214.
- [HL19] Matthew Hedden and Adam Simon Levine, *A surgery formula for knot floer homology*, arXiv preprint arXiv:1901.02488 (2019).
- [HM17] Kristen Hendricks and Ciprian Manolescu, *Involutive Heegaard Floer homology*, *Duke Math. J.* **166** (2017), no. 7, 1211–1299. MR 3649355
- [Juh15] András Juhász, *A survey of Heegaard Floer homology*, *New ideas in low dimensional topology*, Ser. Knots Everything, vol. 56, World Sci. Publ., Hackensack, NJ, 2015, pp. 237–296. MR 3381327
- [Lin20] Francesco Lin, *Indefinite stein fillings and pin (2) -monopole floer homology*, *Selecta Mathematica* **26** (2020), no. 2, 18.
- [OS04a] Peter Ozsváth and Zoltán Szabó, *Holomorphic disks and knot invariants*, *Adv. Math.* **186** (2004), no. 1, 58–116. MR 2065507
- [OS04b] ———, *Holomorphic disks and topological invariants for closed three-manifolds*, *Ann. of Math. (2)* **159** (2004), no. 3, 1027–1158. MR 2113019
- [OS05] ———, *On knot Floer homology and lens space surgeries*, *Topology* **44** (2005), no. 6, 1281–1300. MR 2168576
- [OS06] ———, *Lectures on Heegaard Floer homology*, *Floer homology, gauge theory, and low-dimensional topology*, *Clay Math. Proc.*, vol. 5, Amer. Math. Soc., Providence, RI, 2006, pp. 29–70. MR 2249248
- [OS11] ———, *Knot Floer homology and rational surgeries*, *Algebr. Geom. Topol.* **11** (2011), no. 1, 1–68. MR 2764036
- [Rac15] Bela Andras Racz, *Geometry of $(1,1)$ -Knots and Knot Floer Homology*, ProQuest LLC, Ann Arbor, MI, 2015, Thesis (Ph.D.)–Princeton University. MR 3337599
- [Ras03] Jacob Rasmussen, *Floer homology and knot complements*, ProQuest LLC, Ann Arbor, MI, 2003, Thesis (Ph.D.)–Harvard University. MR 2704683
- [Ras05] ———, *Knot polynomials and knot homologies*, *Geometry and topology of manifolds*, *Fields Inst. Commun.*, vol. 47, Amer. Math. Soc., Providence, RI, 2005, pp. 261–280. MR 2189938
- [RR17] Jacob Rasmussen and Sarah Dean Rasmussen, *Floer simple manifolds and L -space intervals*, *Adv. Math.* **322** (2017), 738–805. MR 3720808
- [Zem19] Ian Zemke, *Connected sums and involutive knot Floer homology*, *Proc. Lond. Math. Soc. (3)* **119** (2019), no. 1, 214–265. MR 3957835
- [Zho21] Hugo Zhou, *Homology concordance and an infinite rank free subgroup*, *J. Topol.* **14** (2021), no. 4, 1369–1395. MR 4406694

DEPARTMENT OF MATHEMATICS, BOSTON COLLEGE, CHESTNUT HILL, MA, USA
Email address: binnsf@bc.edu

SCHOOL OF MATHEMATICS, GEORGIA INSTITUTE OF TECHNOLOGY, ATLANTA, GA, USA
Email address: hzhou@gatech.edu